

# Learning-based Attitude Estimation with Noisy Measurements and Unknown Gyro Bias

Parham Oveissi, Mohammad Mirtaba, Ankit Goel

**Abstract**— This paper introduces a learning-based, data-driven attitude estimator, called the retrospective cost attitude estimator (RCAE), for the  $SO(3)$  attitude representation. RCAE is motivated by the multiplicative extended Kalman filter (MEKF). However, unlike MEKF, which requires computing a Jacobian to compute the correction signal, RCAE uses retrospective cost optimization that depends only on the measured data. Moreover, due to the structure of the correction signal, RCAE does not require explicit estimation of gyro bias. The performance of RCAE is verified and compared with MEKF through both numerical simulations and physical experiments.

**keywords:** attitude estimation, attitude filtering, Kalman filter, adaptive estimation, learning-based estimation, data-driven attitude estimation.

## I. INTRODUCTION

Attitude estimation, also known as orientation estimation, is a pivotal technology widely used in applications across several domains, including aerospace, robotics, computer vision, and navigation. The primary objective of attitude estimation is to ascertain the orientation of an object in three-dimensional space relative to a reference frame. In many real-world applications, attitude estimation is a critical enabling technology. For example, it is essential in inertial navigation systems, enabling vehicles to navigate in unknown environments [1], [2]. Robotic agents use attitude estimation to comprehend their spatial orientation, facilitating effective interaction with their surroundings [3]. Furthermore, with advancements in computational technology and resources, attitude estimation is crucial for augmented reality experiences, 3D reconstruction, and object tracking [4].

Attitude estimation is a special case of the state estimation problem in dynamic systems. In general, state estimation techniques involve the propagation of the state estimate using a model of the dynamic system and a correction of the state estimate using a system measurement. Kalman filter is the most well-known state

estimation technique that applies to linear systems [5], [6]. Various extensions of the Kalman filter for nonlinear systems have been developed, such as the Extended Kalman Filter (EKF), Ensemble Kalman Filter (EnKF), Unscented Kalman Filter (UKF), and Particle filters [7].

In addition to the nonlinearity of the attitude dynamics, the attitude estimation problem is further complicated by the special geometric structure of the mathematical representation of the attitude. The attitude of a rigid body can be parameterized by a  $3 \times 3$  direction cosine matrix (DCM), a four-dimensional quaternion vector, or three Euler angles, etc. [8]. Each of these parameterizations entails some trade-offs. The DCM, an element of  $SO(3)$ , is unique for a given attitude but consists of nine real numbers. A quaternion, an element of  $S^3$ , consists of four real numbers but suffers from non-uniqueness. Euler angles uniquely determine the attitude but suffer from singularities, known as the gimbal lock problem [1].

Variations of the Kalman filter have been applied to the attitude estimation problem with DCM and quaternion parameterization. However, the additive step in the Kalman filter, also known as the *data assimilation* step, often produces an estimate that violates the geometric structure of the representation [9], [10]. [11] proposed the Multiplicative Extended Kalman Filter (MEKF) with quaternion parameterization, replacing the additive state correction step with a multiplicative step, thus preserving the geometric structure of the quaternion. In [12]–[14], the multiplicative technique was developed for the  $3 \times 3$  DCM.

In all of these techniques, the computation of the Kalman gain is computationally expensive, requiring the propagation of the corresponding covariance matrix [15]. To address this, we present a novel attitude estimator called the Retrospective Cost Attitude Estimator (RCAE). More details on MEKF can be found in [9], [11], [12].

Like the MEKF, RCAE corrects the attitude estimate with a multiplicative correction, preserving the geometric structure of the attitude parameterization. However, unlike MEKF, the multiplicative correction signal in RCAE is computed using a learning-based approach involving retrospective cost optimization and measured data. RCAE leverages the retrospective cost

Parham Oveissi is a graduate student in the Department of Mechanical Engineering, University of Maryland, Baltimore County, 1000 Hilltop Circle, Baltimore, MD 21250. parhamo1@umbc.edu

Mohammad Mirtaba is a graduate student in the Department of Mechanical Engineering, University of Maryland, Baltimore County, 1000 Hilltop Circle, Baltimore, MD 21250. mmirtaba@umbc.edu

Ankit Goel is an Assistant Professor in the Department of Mechanical Engineering, University of Maryland, Baltimore County, 1000 Hilltop Circle, Baltimore, MD 21250. ankgoe1@umbc.edu

optimization technique [16] and is motivated by retrospective cost adaptive control (RCAC). RCAC is a data-driven, learning-based adaptive control technique applicable to stabilization, tracking, and disturbance rejection problems and has been applied to various engineering problems [17]–[21]. RCAE is computationally efficient since the attitude correction signal is scalar instead of a vector, as in MEKF. Furthermore, the correction signal is updated by a recursive retrospective cost optimization algorithm which is driven by measured data, eliminating the need for Jacobian computations. Additionally, unlike Kalman filter-based techniques, where an unknown gyro bias requires explicit estimation, RCAE can reject the effect of unknown gyro bias without modifying the algorithm.

The paper is organized as follows. Section II formulates the attitude estimation problem. The retrospective cost attitude estimator is presented in Section III. In Section IV, RCAE is implemented and validated in a numerical experiment as well as a physical experimental setup. Finally, the paper concludes in Section V with a discussion of future work.

## II. PROBLEM FORMULATION

Let  $F_A = (\hat{i}_A, \hat{j}_A, \hat{k}_A)$  be an inertial frame, where  $\hat{i}_A, \hat{j}_A, \hat{k}_A$  are mutually orthonormal vectors. Let  $\mathcal{B}$  be a rigid body and let  $F_B = (\hat{i}_B, \hat{j}_B, \hat{k}_B)$  be a frame fixed to  $\mathcal{B}$ . Let the *orientation matrix*  $\mathcal{O}_{B/A}(t) \in SO(3) \subset \mathbb{R}^{3 \times 3}$  denote the attitude of  $F_B$  relative to  $F_A$  at time  $t$ . Note that the orientation matrix  $\mathcal{O}_{B/A}$  is the transpose of the direction cosine matrix. Letting  $\omega_{B/A|B}(t) \in \mathbb{R}^3$  denote that angular velocity vector of  $F_B$  relative  $F_A$  with respect to the frame  $F_B$  at time  $t$ , it follows from the Poisson's equation [8] that the orientation matrix satisfies

$$\dot{\mathcal{O}}_{B/A}(t) = -\omega_{B/A|B}(t)^\times \mathcal{O}_{B/A}(t). \quad (1)$$

where, for  $x \in \mathbb{R}^3$ ,

$$x^\times \triangleq \begin{bmatrix} 0 & -x_3 & x_2 \\ x_3 & 0 & -x_1 \\ -x_2 & x_1 & 0 \end{bmatrix}. \quad (2)$$

The orientation of  $\mathcal{B}$  can thus be obtained by integrating the Poisson's equation (1), which yields

$$\mathcal{O}_{B/A}(t) = e^{-\int_0^t \omega_{B/A|B}(t)^\times dt} \mathcal{O}_{B/A}(0). \quad (3)$$

Note that if the angular velocity vector is time-varying, the computation of the integral in (3) is an intractable problem. Several integration techniques to integrate (1) are discussed in [22]–[27]. However, since the attitude dynamics, given by (1), lacks dissipation, if the initial orientation  $\mathcal{O}_{B/A}(0)$  is not precisely known, then the error in the orientation matrix computed by integrating (1) does not converge to zero.

Instead of continuous-time integration, which may be intractable, the orientation matrix can be discretely propagated, as shown below. If, for  $\tau \in [t, t + \Delta t]$ ,  $\omega_{B/A|B}(\tau) = \omega \hat{n}$ , where  $\omega \in \mathbb{R}$  and  $\hat{n} \in \mathbb{R}^3$ , then

$$\mathcal{O}_{B/A}(t + \Delta t) = e^{-\omega \Delta t \hat{n}^\times} \mathcal{O}_{B/A}(t). \quad (4)$$

In the case where the direction of the angular velocity vector changes slowly or the time step  $\Delta t$  is sufficiently small, the orientation of  $\mathcal{B}$  can be computed using (4). However, the computed orientation matrix may not necessarily represent the attitude of  $\mathcal{B}$  due to discretization error in numerical integration. Furthermore, if the measurement of the angular velocity vector is noisy, then the orientation matrix, computed by integrating (1), is erroneous.

In this work, we assume that a noisy measurement of the orientation  $\mathcal{O}_{B/A}$  is available. The noisy orientation measurement is denoted by  $\mathcal{O}_{B_m/A}$ . In the physical experiment, a noisy measurement of the orientation  $\mathcal{O}_{B/A}$  is computed using the IMU data. The details of the orientation computation are described in Appendix I. Alternatively, the orientation measurements can be obtained using vision-based sensors [28]–[30].

The problem is to develop an attitude estimator that combines the orientation propagation and a noisy measurement of the orientation to construct a more accurate estimate of the attitude.

## III. RETROSPECTIVE COST ATTITUDE ESTIMATOR

This section presents the data-driven retrospective cost attitude estimator (RCAE). The attitude estimator is motivated by the multiplicative extended Kalman filter (MEKF).

### A. Attitude Error

Following the definition of the attitude error in [11], [14], [31], we define the attitude error  $z \in \mathbb{R}$  between two orientation matrices  $\mathcal{O}_1$  and  $\mathcal{O}_2$  as

$$z \triangleq \text{tr}(\mathcal{O}_1^T \mathcal{O}_2 - I_3), \quad (5)$$

where  $I_3$  is the  $3 \times 3$  identity matrix. Note that if  $\mathcal{O}_1 = \mathcal{O}_2$ , then  $z = 0$ . Note that  $z \in [-4, 0]$ .

For  $k = \{1, 2, \dots\}$ , let  $\mathcal{O}_{B/A}^k$  denote the orientation  $\mathcal{O}_{B/A}(k\Delta_T)$  at time  $t = k\Delta_T$ . Let  $\hat{\mathcal{O}}_{B/A}^k$  and  $\mathcal{O}_{B_m/A}^k$  denote an estimate and a measurement of the orientation  $\mathcal{O}_{B/A}^k$ , respectively at step  $k$ . Then,

$$\mathcal{O}_{\hat{B}/B_m}^k = \hat{\mathcal{O}}_{B/A}^k \mathcal{O}_{A/B_m}^k = \hat{\mathcal{O}}_{B/A}^k (\mathcal{O}_{B_m/A}^k)^T. \quad (6)$$

Define the error

$$z_k \triangleq \text{tr}(\mathcal{O}_{\hat{B}/B_m}^k - I_3). \quad (7)$$

## B. Attitude Estimator

The retrospective cost attitude estimator is

$$\mathcal{O}_{\hat{B}/A}^{k+1} = e^{-(\omega_k \Delta T + \eta_k)^\times} \mathcal{O}_{\hat{B}/A}^k, \quad (8)$$

where  $\omega_k \triangleq \omega_{B/A|B}(k\Delta t)$ , and the *attitude correction signal*  $\eta_k \in \mathbb{R}^3$  is given by

$$\eta_k = u_k n_{\hat{B}/B_m}^k, \quad (9)$$

where  $n_{\hat{B}/B_m}^k \in \mathbb{R}^3$  is the eigenaxis of the orientation matrix  $\mathcal{O}_{\hat{B}/B_m}^k$ , and the signal  $u_k \in \mathbb{R}$  is computed using the retrospective cost optimization described in the next section. Note that

$$n_{\hat{B}/B_m}^k = \frac{1}{2 \sin \theta_{\hat{B}/B_m}^k} (\mathcal{O}_{\hat{B}/B_m}^k - \mathcal{O}_{B_m/\hat{B}}^k)^{-\times}. \quad (10)$$

## C. Retrospective Cost Optimization

This section briefly reviews retrospective cost adaptive control (RCAC) and focuses on the algorithm for the attitude estimation problem. RCAC is described in detail in [32], and its extension to digital PID control is given in [33]. Consider a system

$$x_{k+1} = f(k, x_k, u_k, w_k), \quad (11)$$

$$z_k = g(k, x_k, w_k), \quad (12)$$

where  $x_k$  is the state,  $u_k$  is the input,  $w_k$  is the exogenous signal that can represent commands, external disturbance, or both, and  $z_k$  is the performance variable. The functions  $f$  and  $g$  represent the dynamics and output maps. The goal is to develop an adaptive law that drives the performance variable  $z_k$  to zero, asymptotically to zero without explicit knowledge of  $f$  and  $g$ .

Consider an adaptive law

$$u_k = \Phi_k \theta_k, \quad (13)$$

where  $\Phi_k \in \mathbb{R}^{l_u \times l_\theta}$  is the regressor matrix that is constructed using measurements and  $\theta_k \in \mathbb{R}^{l_\theta}$  is the vector of the gains optimized by RCAC at step  $k$ . For example, a discrete-time adaptive PID update law can be written in the form given by (13), where, at step  $k$ ,

$$\Phi_k \triangleq [z_k \quad \gamma_k \quad z_k - z_{k-1}], \quad \theta_k = \begin{bmatrix} K_{p,k} \\ K_{i,k} \\ K_{d,k} \end{bmatrix}, \quad (14)$$

$\gamma_k = \sum_i z_i$  is the accumulated error, and  $K_{p,k}$ ,  $K_{i,k}$ , and  $K_{d,k}$  are the proportional, integral, and derivative gains, respectively. Various MIMO parameterizations of the adaptive law (13) are described in [34]. To determine the gains  $\theta_k$ , let  $\theta \in \mathbb{R}^{l_\theta}$ , define the *retrospective performance variable* by

$$\hat{z}_k(\theta) \triangleq z_k + G_f(\mathbf{q})(\Phi_k \theta - u_k), \quad (15)$$

where

$$G_f(\mathbf{q}) \triangleq \sum_{i=1}^{n_f} \frac{N_i}{\mathbf{q}^i} \quad (16)$$

is an FIR filter. Note that  $N_i \in \mathbb{R}^{l_z \times l_u}$ . Furthermore, define the *retrospective cost function*  $J_k: \mathbb{R}^{l_\theta} \rightarrow [0, \infty)$  by

$$J_k(\theta) \triangleq \sum_{i=0}^k \hat{z}_i(\theta)^\top R_z \hat{z}_i(\theta) + (\Phi_k \theta)^\top R_u (\Phi_k \theta) + (\theta - \theta_0)^\top P_0^{-1} (\theta - \theta_0), \quad (17)$$

where  $R_z \in \mathbb{R}^{l_z \times l_z}$ ,  $R_u \in \mathbb{R}^{l_u \times l_u}$ , and  $P_0 \in \mathbb{R}^{l_\theta \times l_\theta}$  are positive definite; and  $\theta_0 \in \mathbb{R}^{l_\theta}$  is the initial vector of controller gains.

*Proposition 3.1:* Consider (17), where  $\theta_0 \in \mathbb{R}^{l_\theta}$  and  $P_0 \in \mathbb{R}^{l_\theta \times l_\theta}$  is positive definite. For all  $k \geq 0$ , denote the minimizer of  $J_k$  given by (17) by

$$\theta_{k+1} \triangleq \underset{\theta \in \mathbb{R}^{l_\theta}}{\operatorname{argmin}} J_k(\theta). \quad (18)$$

Then, for all  $k \geq 0$ ,  $\theta_{k+1}$  is given by

$$\begin{aligned} \theta_{k+1} &= \theta_k - P_{k+1} \Phi_{f,k}^\top R_z (z_k + \Phi_{f,k} \theta_k - u_{f,k}) \\ &\quad - P_{k+1} \Phi_k^\top R_u \Phi_k \theta_k, \end{aligned} \quad (19)$$

where

$$P_{k+1} = P_k - P_k \bar{\Phi}_k^\top \left( \bar{R}^{-1} + \bar{\Phi}_k P_k \bar{\Phi}_k^\top \right)^{-1} \bar{\Phi}_k P_k, \quad (20)$$

and

$$\Phi_{f,k} \triangleq G_f(\mathbf{q}) \Phi_k, \quad u_{f,k} \triangleq G_f(\mathbf{q}) u_k, \quad (21)$$

$$\bar{\Phi}_k \triangleq \begin{bmatrix} \Phi_{f,k} \\ \Phi_k \end{bmatrix}, \quad \bar{R} \triangleq \begin{bmatrix} R_z & 0 \\ 0 & R_u \end{bmatrix}. \quad (22)$$

*Proof:* See [35], [36].  $\blacksquare$

Finally, the adaptive signal at step  $k+1$  is given by

$$u_{k+1} = \Phi_{k+1} \theta_{k+1}. \quad (23)$$

In the attitude estimation problem, the performance variable  $z_k$  is given by (7). Note that both  $z_k$  and the adaptive signal  $u_k$  are scalars. The RCAE is thus (8), (9), (13), (19), and (20), and its architecture is shown in Figure 1.

## IV. EXPERIMENTAL VERIFICATION AND PERFORMANCE COMPARISON

In this section, we apply the RCAE developed in the previous section to estimate the attitude of a rigid body with a noisy angular velocity and attitude measurement in a numerical simulation as well as a physical experiment. Furthermore, the performance of RCAE is also compared with MEKF

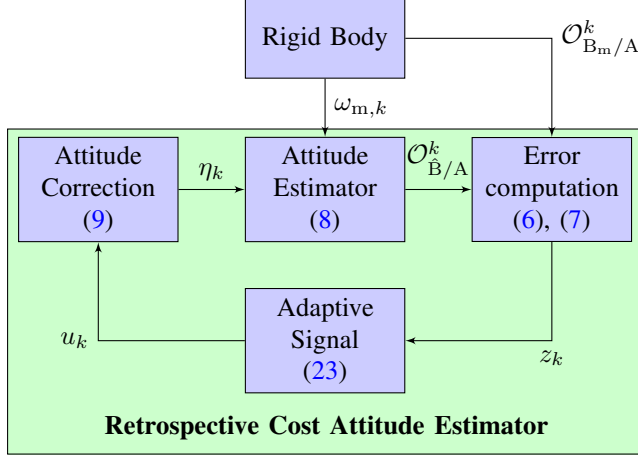


Fig. 1: Retrospective cost attitude estimator architecture.

### A. Numerical Simulation

The rigid body  $\mathcal{B}$  is assumed to be rotating with a time-varying angular velocity vector given by

$$\omega_{\mathcal{B}/\mathcal{A}}(t) = \begin{bmatrix} 80 \cos(5.0t) \\ 60 \cos(7.0t) \\ 40 \cos(9.0t) \end{bmatrix}. \quad (24)$$

The 3-2-1 Euler angles  $\psi$ ,  $\theta$ , and  $\phi$  corresponding to the orientation matrix of  $\mathcal{B}$  at  $t = 0$ , in degrees, are assumed to be

$$\psi(0) = 30, \quad \theta(0) = 20, \quad \phi(0) = 10. \quad (25)$$

The initial orientation is thus

$$\mathcal{O}_{\mathcal{B}/\mathcal{A}}(0) = \mathcal{O}_1(10)\mathcal{O}_2(20)\mathcal{O}_3(30), \quad (26)$$

where  $\mathcal{O}_1(\phi)$ ,  $\mathcal{O}_2(\theta)$ , and  $\mathcal{O}_3(\psi)$  are the Euler matrices corresponding to the rotation by  $\phi$ ,  $\theta$ , and  $\psi$  degrees about the first, second, and third Euler axis, respectively. In this work, we simulate the orientation  $\mathcal{O}_{\mathcal{B}/\mathcal{A}}(t)$  by discretely propagating (4).

The measured angular velocity vector is assumed to be

$$\omega_{m,k} = \omega_k + b + w_k, \quad (27)$$

where  $\omega_k \triangleq \omega_{\mathcal{B}/\mathcal{A}}(k\Delta t)$ ,  $b \in \mathbb{R}^3$  is an unknown bias and  $w_k \sim \mathcal{N}(0, \sigma_w^2 I_3)$  is a zero-mean Gaussian noise. In this example, we set  $b = [5 \ 7 \ 4]^T$  and  $\sigma_w = 2$  deg/sec. Figure 2 shows the true and measured angular velocity.

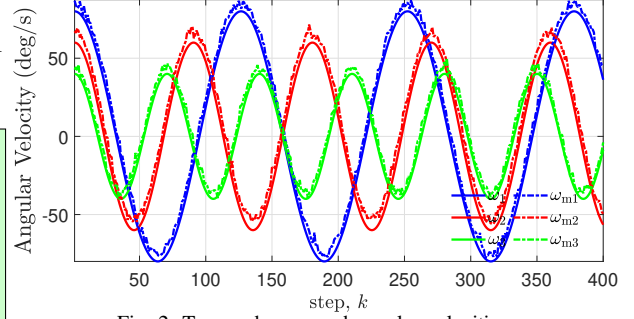


Fig. 2: True and measured angular velocities.

The orientation measurements are constructed as follows. Let  $\phi_k$ ,  $\theta_k$ , and  $\psi_k$  denote the 3-2-1 Euler angles of  $\mathcal{O}_{\mathcal{B}/\mathcal{A}}(k\Delta t)$ . The measured orientation is then given by

$$\mathcal{O}_{\mathcal{B}_m/\mathcal{A}}^k = \mathcal{O}_1(\phi_{m,k})\mathcal{O}_2(\theta_{m,k})\mathcal{O}_3(\psi_{m,k}), \quad (28)$$

where

$$\begin{bmatrix} \phi_{m,k} \\ \theta_{m,k} \\ \psi_{m,k} \end{bmatrix} = \begin{bmatrix} \phi_k \\ \theta_k \\ \psi_k \end{bmatrix} + v_k, \quad (29)$$

and  $v_k \sim \mathcal{N}(0, \sigma_v^2 I_3)$  is a zero-mean Gaussian noise. In this example, we set  $\sigma_v = 5$  deg.

In RCAE, we set  $N_1 = 1$ ,  $P_0 = 0.1I_3$ ,  $\lambda = 1$ . The initial attitude estimate  $\mathcal{O}_{\mathcal{B}/\mathcal{A}}^0 = I_3$  since no prior information about the attitude is assumed. Figure 3 shows the 3-2-1 Euler angles corresponding to the true orientation  $\mathcal{O}_{\mathcal{B}/\mathcal{A}}^k$ , measured orientation  $\mathcal{O}_{\mathcal{B}_m/\mathcal{A}}^k$ , and estimation orientation  $\mathcal{O}_{\mathcal{B}/\mathcal{A}}^k$ . Figure 4 shows a) the signal  $u_k$  computed by RCAE, and b) the estimator gain  $\theta_k$  computed by RCAE. Figure 5 shows the true and estimated frames corresponding to the true orientation  $\mathcal{O}_{\mathcal{B}/\mathcal{A}}^k$ , and estimation orientation  $\mathcal{O}_{\mathcal{B}/\mathcal{A}}^k$  at several iteration steps during the estimation.

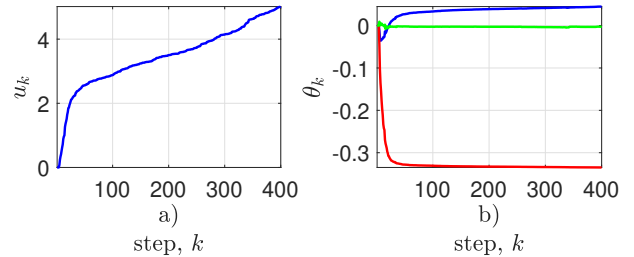


Fig. 4: Retrospective cost attitude estimation. a) shows the signal  $u_k$  computed by RCAE, and b) shows the estimator gain  $\theta_k$  optimized by RCAE.

Next, the attitude is estimated using MEKF, where the attitude is represented as a quaternion. In MEKF, we set the initial covariance of quaternion error  $P(0) = 10^4 I_6$ , the process covariance  $Q = \begin{bmatrix} 0.0001 I_3 & 0 \\ 0 & I_3 \end{bmatrix}$  and

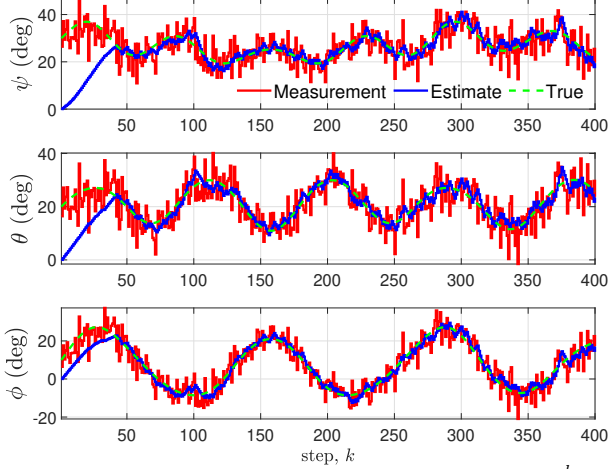


Fig. 3: 3-2-1 Euler angles corresponding to the true orientation  $\mathcal{O}_{B/A}^k$ , measured orientation  $\mathcal{O}_{B_m/A}^k$ , and estimated orientation  $\mathcal{O}_{\hat{B}/A}^k$  using RCAE.

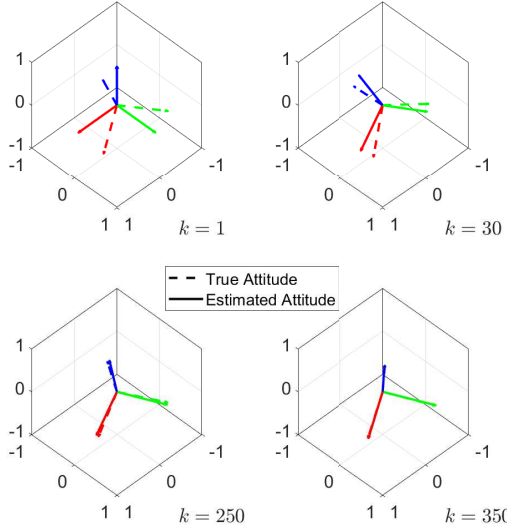


Fig. 5: True and estimated frames corresponding to the true orientation  $\mathcal{O}_{B/A}^k$  and estimated orientation  $\mathcal{O}_{\hat{B}/A}^k$ .

the measurement covariance  $R = \begin{bmatrix} 0.01I_3 & 0 \\ 0 & 100I_3 \end{bmatrix}$ . Since MEKF provides the estimate of the attitude in the quaternion form, we convert the attitude estimate to the orientation matrix and the corresponding 3-2-1 Euler angles. In particular, the orientation matrix  $\mathcal{O}_{B/A}$  corresponding to the quaternion

$$q_{B/A} = \begin{bmatrix} \eta_{B/A} \\ \varepsilon_{B/A} \end{bmatrix}, \quad (30)$$

where  $\eta_{B/A} \in [-1, 1]$  and  $\varepsilon_{B/A} \in \mathbb{R}^3$  is

$$\mathcal{O}_{B/A} = I_3 - 2\eta_{B/A}\varepsilon_{B/A}^\times + 2\varepsilon_{B/A}^{\times 2}. \quad (31)$$

Figure 6 shows the attitude error  $z_k$  computed with both MEKF and RCAE. Figure 7 shows the absolute value of the 3-2-1 Euler angle errors  $e_\psi$ ,  $e_\theta$ , and  $e_\phi$  obtained with MEKF and RCAE. Note that, unlike the MEKF, the RCAE directly estimates the orientation matrix and is computationally less expensive. Additionally, while the MEKF requires explicit estimation and correction of gyro bias, the RCAE can compensate for an unknown constant bias without needing to estimate it.

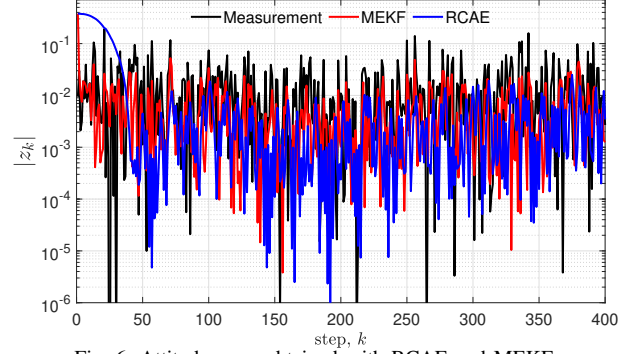


Fig. 6: Attitude error obtained with RCAE and MEKF.

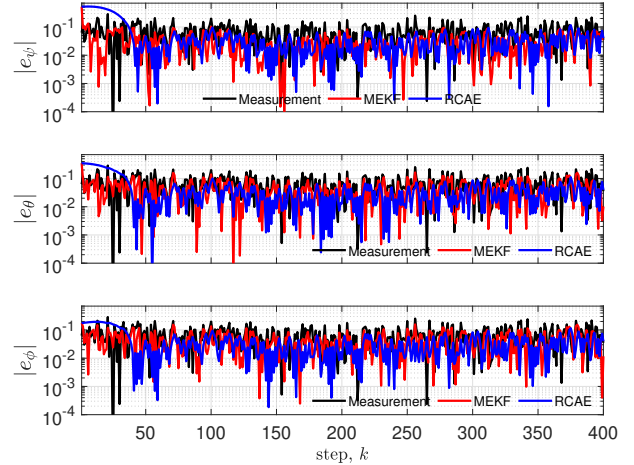


Fig. 7: 3-2-1 Euler angle errors obtained with RCAE and MEKF.

### B. Physical Experiment

To investigate and verify the performance of the RCAE algorithm, an experimental setup featuring a BNO055 sensor is used. The BNO055 is a popular 9-DOF IMU module that integrates a triaxial accelerometer, gyroscope, and magnetometer. It also includes a microcontroller with sensor fusion algorithms, allowing it to provide directly calibrated orientation data (quaternions, Euler angles). In this setup, the raw data from the accelerometer and magnetometer are used to obtain a noisy orientation measurement. In contrast, the orientation data from the BNO055's built-in sensor fusion algorithms serves as the ground truth for performance comparison.

First, the performance of the RCAE algorithm is evaluated using the experimental setup. The gyroscope data is utilized in equation (8) to propagate Poisson's equation, while the raw accelerometer and magnetometer data are used to construct a noisy measurement of  $\mathcal{O}_{B/A}$ , following equations (34), (35) and (36).

Figure 8 shows the 3-2-1 Euler angles corresponding to the true orientation  $\mathcal{O}_{B/A}^k$ , measured orientation  $\mathcal{O}_{B_m/A}^k$ , and estimation orientation  $\mathcal{O}_{\hat{B}/A}^k$ .

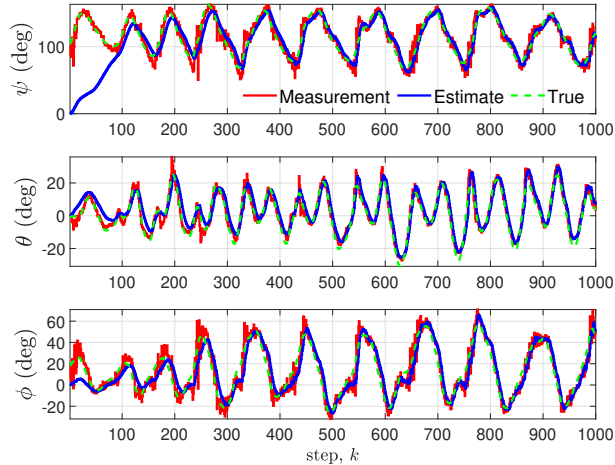


Fig. 8: 3-2-1 Euler angles corresponding to the true orientation  $\mathcal{O}_{B/A}^k$ , measured orientation  $\mathcal{O}_{B_m/A}^k$ , and estimation orientation  $\mathcal{O}_{\hat{B}/A}^k$ . Note that the estimates are closer to the true values of the Euler angles than the measurements.

Figure 9 shows the true and estimated frames corresponding to the true orientation  $\mathcal{O}_{B/A}^k$ , and estimation orientation  $\mathcal{O}_{\hat{B}/A}^k$  at several iteration steps during the estimation.

Next, the attitude is estimated using MEKF, where the attitude is represented as a quaternion. In MEKF, we set the initial covariance of quaternion error  $P(0) = 10^4 I_6$ , the process covariance  $Q = \begin{bmatrix} 0.0001 I_3 & 0 \\ 0 & I_3 \end{bmatrix}$  and the measurement covariance  $R = \begin{bmatrix} 0.01 I_3 & 0 \\ 0 & 100 I_3 \end{bmatrix}$ . A reference gravity vector and magnetic field are also needed, obtained from a fixed accelerometer and the World Magnetic Model (WMM), respectively.

Figure 10 shows the attitude error  $z_k$  computed with both MEKF and RCAE. Figure 11 shows the absolute value of the 3-2-1 Euler angle errors  $e_\psi, e_\theta$ , and  $e_\phi$  obtained with MEKF and RCAE. Note that, unlike the MEKF, the RCAE directly estimates the orientation matrix and is computationally less expensive. Additionally, while the MEKF requires explicit estimation and correction of gyro bias, the RCAE can compensate for an unknown constant bias without needing to estimate it.

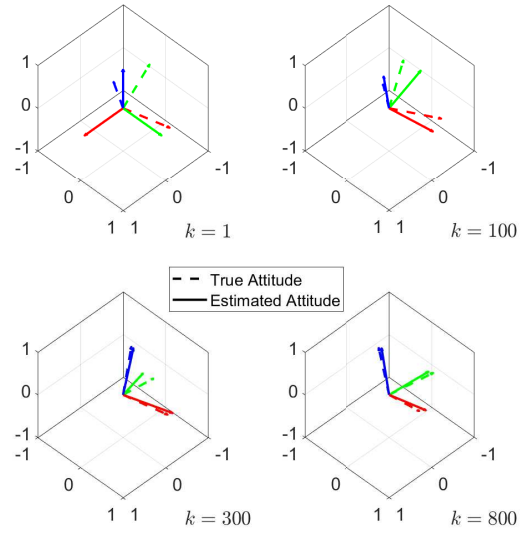


Fig. 9: True and estimated frames corresponding to the true orientation  $\mathcal{O}_{B/A}^k$  and estimation orientation  $\mathcal{O}_{\hat{B}/A}^k$ .

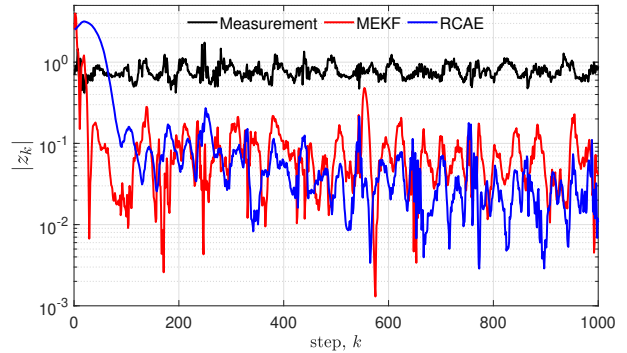


Fig. 10: Attitude error obtained with RCAE and MEKF.

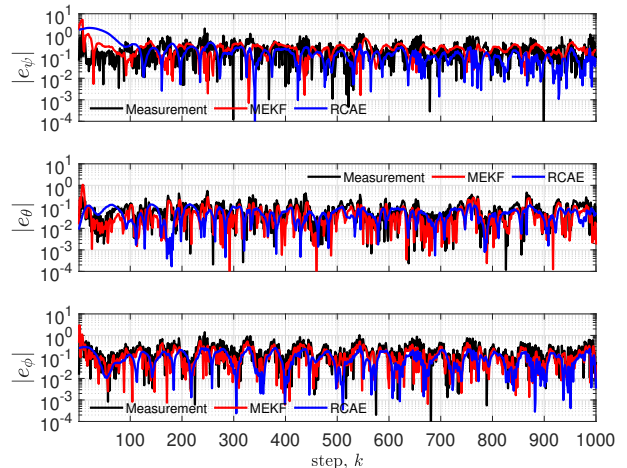


Fig. 11: 3-2-1 Euler angle errors obtained with RCAE and MEKF.

## V. CONCLUSIONS AND FUTURE WORK

This paper presented a novel learning-based attitude estimator with multiplicative correction, leveraging retrospective cost optimization. The estimator, termed the Retrospective Cost Attitude Estimator (RCAE), is specifically developed for the  $3 \times 3$  orientation matrix parameterization of attitude. Unlike traditional Kalman filter-based estimation techniques, RCAE employs a Recursive Least Squares (RLS)-based optimization algorithm that uses only the measured data to learn the appropriate estimator gains, eliminating the need for Jacobian computations and covariance matrix propagation. The efficacy of the proposed estimator is validated through comprehensive numerical experiments and a physical experimental setup. RCAE demonstrates robust performance, accurately estimating attitude while effectively rejecting unknown gyro bias without the need for explicit estimation.

Future work will focus on extending RCAE to quaternion parameterization, and implementing and verifying the retrospective cost attitude estimator in real-world applications such as UAV control and navigation, further demonstrating its practical utility and robustness in dynamic environments.

## REFERENCES

- [1] A. Goel, A. U. Islam, A. Ansari, O. Kouba, and D. S. Bernstein, "An introduction to inertial navigation from the perspective of state estimation [focus on education]," *IEEE Control Systems Magazine*, vol. 41, no. 5, pp. 104–128, 2021.
- [2] M. Mirtaba, M. Jeddi, A. Nikoofard, and Z. Shirmohammadi, "Design and implementation of a low-complexity flight controller for a quadrotor uav," *International Journal of Dynamics and Control*, vol. 11, no. 2, pp. 689–700, 2023.
- [3] S. I. Roumeliotis, G. S. Sukhatme, and G. A. Bekey, "Smoother based 3d attitude estimation for mobile robot localization," in *Proceedings 1999 IEEE International Conference on Robotics and Automation (Cat. No. 99CH36288C)*, IEEE, vol. 3, 1999, pp. 1979–1986.
- [4] D. Xu, M. Xing, X.-G. Xia, G.-C. Sun, J. Fu, and T. Su, "A multi-perspective 3d reconstruction method with single perspective instantaneous target attitude estimation," *Remote Sensing*, vol. 11, no. 11, p. 1277, 2019.
- [5] D. Simon, *Optimal state estimation: Kalman, H infinity, and nonlinear approaches*. John Wiley & Sons, 2006.
- [6] C. K. Chui, G. Chen, et al., *Kalman filtering*. Springer, 2017.
- [7] S. Särkkä and L. Svensson, *Bayesian filtering and smoothing*. Cambridge university press, 2023, vol. 17.
- [8] N. J. Kasdin and D. A. Paley, *Engineering Dynamics: A Comprehensive Introduction*. Princeton University Press, 2011.
- [9] E. J. Lefferts, F. L. Markley, and M. D. Shuster, "Kalman filtering for spacecraft attitude estimation," *Journal of Guidance, control, and dynamics*, vol. 5, no. 5, pp. 417–429, 1982.
- [10] J. L. Crassidis, F. L. Markley, and Y. Cheng, "Survey of nonlinear attitude estimation methods," *Journal of guidance, control, and dynamics*, vol. 30, no. 1, pp. 12–28, 2007.
- [11] F. L. Markley, "Attitude error representations for kalman filtering," *Journal of guidance, control, and dynamics*, vol. 26, no. 2, pp. 311–317, 2003.
- [12] F. L. Markley, "Attitude filtering on so (3)," *The Journal of the Astronautical Sciences*, vol. 54, no. 3-4, pp. 391–413, 2006.
- [13] N. Chatuverdi, A. K. Sanyal, and N. H. McClamroch, "Rigid-body attitude control using rotation matrices for continuous, singularity-free control laws," *IEEE Control Systems Magazine*, vol. 31, no. 8, pp. 30–51, 2011.
- [14] A. H. de Ruiter, "So (3)-constrained kalman filtering with application to attitude estimation," in *2014 American Control Conference*, IEEE, 2014, pp. 4937–4942.
- [15] P. Oveissi, "A novel data-driven attitude estimation: Retrospective cost attitude filtering (rcaf)," M.S. thesis, University of Maryland, Baltimore County, 2024.
- [16] M. A. Santillo and D. S. Bernstein, "Adaptive control based on retrospective cost optimization," *Journal of guidance, control, and dynamics*, vol. 33, no. 2, pp. 289–304, 2010.
- [17] P. Oveissi, A. Goel, O. Tumuklu, and K. M. Hanquist, "Adaptive combustion regulation in solid fuel ramjet," in *AIAA SCITECH 2024 Forum*, 2024, p. 0743.
- [18] A. Goel, J. A. Paredes, H. Dadhaniya, S. A. U. Islam, A. M. Salim, S. Ravela, and D. Bernstein, "Experimental implementation of an adaptive digital autopilot," in *2021 American Control Conference (ACC)*, IEEE, 2021, pp. 3737–3742.
- [19] Y. Y. Chee, P. Oveissi, J. Paredes, D. S. Bernstein, and A. Goel, "Performance comparison of adaptive autopilot architectures for multicopter stabilization and trajectory tracking," in *AIAA SCITECH 2024 Forum*, 2024, p. 1391.
- [20] P. Oveissi, A. Trivedi, A. Goel, O. Tumuklu, K. M. Hanquist, A. Farahmandi, and D. Philbrick, "Learning-based adaptive thrust regulation of solid fuel ramjet," in *AIAA SCITECH 2023 Forum*, 2023, p. 2533.
- [21] N. Poudel, A. Trivedi, P. Oveissi, M. Yu, A. Goel, and J. T. Hryniuk, "Learning-based adaptive gust mitigation with oscillating wings," in *AIAA SCITECH 2023 Forum*, 2023, p. 0275.
- [22] E. Hairer, C. Lubich, and G. Wanner, *Geometric Numerical Integration: Structure-Preserving Algorithms for Ordinary Differential Equations*. Springer, 2006.
- [23] P. Betsch and R. Siebert, "Rigid body dynamics in terms of quaternions: Hamiltonian formulation and conserving numerical integration," *Int. J. Num. Meth. Eng.*, vol. 79, no. 4, pp. 444–473, 2009.
- [24] F. Zhao and B. Van Wachem, "A novel quaternion integration approach for describing the behaviour of non-spherical particles," *Acta Mechanica*, vol. 224, no. 12, pp. 3091–3109, 2013.
- [25] S. Leyendecker, J. E. Marsden, and M. Ortiz, "Variational integrators for constrained dynamical systems," *ZAMM-J. Applied Mathematics and Mechanics/Zeitschrift für Angewandte Mathematik und Mechanik: Applied Mathematics and Mechanics*, vol. 88, no. 9, pp. 677–708, 2008.
- [26] A. M. Sabatini, "Quaternion-based strap-down integration method for applications of inertial sensing to gait analysis," *Medical and Biological Eng. and Computing*, vol. 43, no. 1, pp. 94–101, 2005.
- [27] S. A. Whitmore, *Closed-form Integrator for the Quaternion (Euler Angle) Kinematics Equations*, US Patent 6,061,611, May 2000.
- [28] A. E. R. Shabayek, C. Demonceaux, O. Morel, and D. Fofi, "Vision based uav attitude estimation: Progress and insights," *Journal of Intelligent & Robotic Systems*, vol. 65, pp. 295–308, 2012.
- [29] S. Thurrowgood, D. Soccol, R. J. Moore, D. Bland, and M. V. Srinivasan, "A vision based system for attitude estimation of uavs," in *2009 IEEE/RSJ International Conference on Intelligent Robots and Systems*, IEEE, 2009, pp. 5725–5730.
- [30] C. Kessler, C. Ascher, N. Frietsch, M. Weinmann, and G. F. Trommer, "Vision-based attitude estimation for indoor navigation using vanishing points and lines," in *IEEE/ION Position, Location and Navigation Symposium*, IEEE, 2010, pp. 310–318.
- [31] P. Oveissi and A. Goel, "Retrospective cost attitude filtering with noisy measurements and unknown gyro bias," *arXiv preprint arXiv:2401.13092*, 2024.
- [32] Y. Rahman, A. Xie, and D. S. Bernstein, "Retrospective Cost Adaptive Control: Pole Placement, Frequency Response, and

- Connections with LQG Control,” *IEEE Control System Magazine*, vol. 37, pp. 28–69, Oct. 2017.
- [33] M. Kamaldar, S. A. U. Islam, S. Sanjeevini, A. Goel, J. B. Hoagg, and D. S. Bernstein, “Adaptive digital PID control of first-order-lag-plus-dead-time dynamics with sensor, actuator, and feedback nonlinearities,” *Advanced Control for Applications*, vol. 1, no. 1, e20, 2019.
- [34] A. Goel, S. A. U. Islam, and D. S. Bernstein, “Adaptive Control of MIMO Systems Using Sparsely Parameterized Controllers,” in *2020 American Control Conference (ACC)*, Jul. 2020, pp. 5340–5345.
- [35] S. A. U. Islam and D. S. Bernstein, “Recursive Least Squares for Real-Time Implementation,” *IEEE Control Systems Magazine*, vol. 39, no. 3, pp. 82–85, Jun. 2019.
- [36] A. Goel, A. L. Bruce, and D. S. Bernstein, “Recursive least squares with variable-direction forgetting: Compensating for the loss of persistency [lecture notes],” *IEEE Control Systems Magazine*, vol. 40, no. 4, pp. 80–102, 2020.

## APPENDIX I ATTITUDE MEASUREMENT

The orientation matrix corresponding to the attitude of  $\mathcal{B}$  can be constructed using direct onboard measurements. Several methods exist to construct the orientation matrix from measured data. For example, vision-based sensors can be used to compute an orientation measurement as described in [28]–[30], or an accelerometer and the magnetometer measurements from an IMU can be used to compute an orientation measurement as described below.

We use the following fact to compute the orientation using the measurements from an IMU.

*Fact 1.1:* Let  $F_A$  and  $F_B$  be two frames. Let  $\vec{x}$  be a vector. Let  $\vec{x}|_A$  and  $\vec{x}|_B$  denote the coordinates of  $\vec{x}$  in frames  $F_A$  and  $F_B$ , respectively. Then,

$$\vec{x}|_B = \mathcal{O}_{B/A} \vec{x}|_A, \quad (32)$$

where  $\mathcal{O}_{B/A}$  is the orientation matrix. Furthermore, it follows from (32) that

$$\mathcal{O}_{B/A} = \begin{bmatrix} \hat{i}_A|_B & \hat{j}_A|_B & \hat{k}_A|_B \end{bmatrix}. \quad (33)$$

Let  $F_A$  be defined such that  $\hat{k}_A$  is aligned with the direction of gravity, that is,  $\vec{g} = g\hat{k}_A$ , and the magnetic field is in the  $\hat{i}_A - \hat{k}_A$  plane. Let  $a \in \mathbb{R}^3$  denote the acceleration measurement. Assuming that the body  $\mathcal{B}$  is not accelerating, the acceleration measurement  $a \approx \vec{g}|_B$ , which implies that

$$\hat{k}_A|_B = \frac{a}{\|a\|}. \quad (34)$$

Next, Let  $m \in \mathbb{R}^3$  denote the magnetic field measurements. Since  $\vec{m}$  is assumed to be in the  $\hat{i}_A - \hat{k}_A$  plane and, for all  $\alpha, \beta \in \mathbb{R}$ ,  $\hat{k}_A \times (\alpha\hat{i}_A + \beta\hat{k}_A) = \alpha\hat{j}_A$ , it follows that

$$\hat{j}_A|_B = \hat{k}_A|_B \times \frac{m}{\|m\|} = \frac{a}{\|a\|} \times \frac{m}{\|m\|} \quad (35)$$

and

$$\hat{i}_A|_B = \hat{k}_A|_B \times \hat{j}_A|_B = \frac{a}{\|a\|} \times \left( \frac{a}{\|a\|} \times \frac{m}{\|m\|} \right). \quad (36)$$

The orientation matrix  $\mathcal{O}_{B/A}$  is finally given by (33) using  $\hat{i}_A|_B$ ,  $\hat{j}_A|_B$ , and  $\hat{k}_A|_B$  computed above.